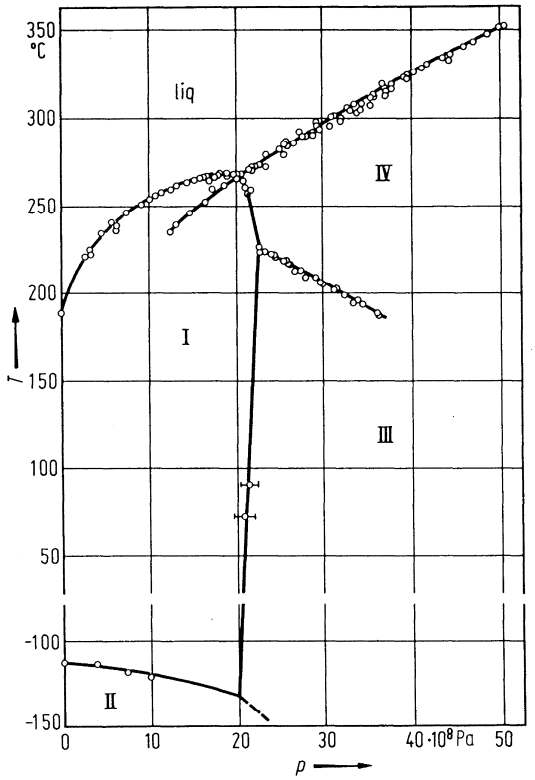

Fig. 33A-5-001. $NH_4H_2PO_4$ (ADP). Phase diagram [69Cla].

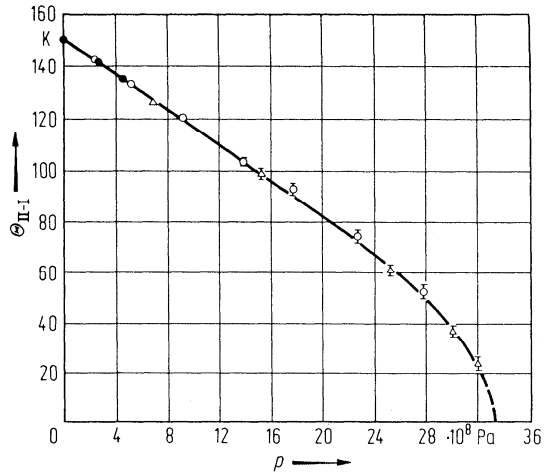

Fig. 33A-5-002. $NH_4H_2PO_4$ (ADP). Θ_{II-I} vs. p [71Sam].

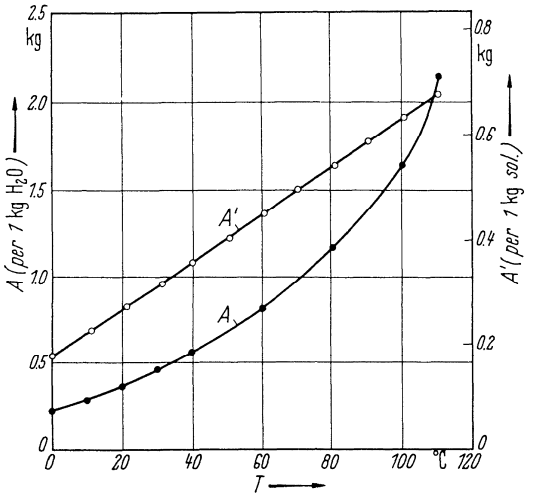

Fig. 33A-5-003. $NH_4H_2PO_4$ (ADP). A, A' vs. T [58Oga]. A and A': mass of ADP soluble in 1 kg H_2O and 1 kg aqueous solution, respectively.

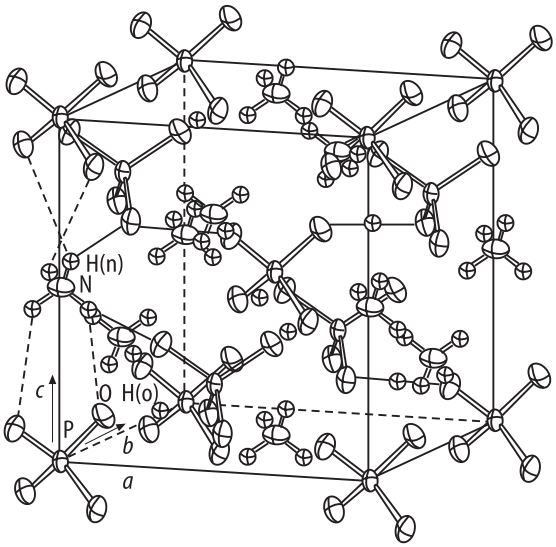

Fig. 33A-5-004. $NH_4H_2PO_4$ (ADP). A perspective view of the unit cell [73Kha]. H(n): H atoms in NH_4 group. H(o): H atoms between two O atoms.

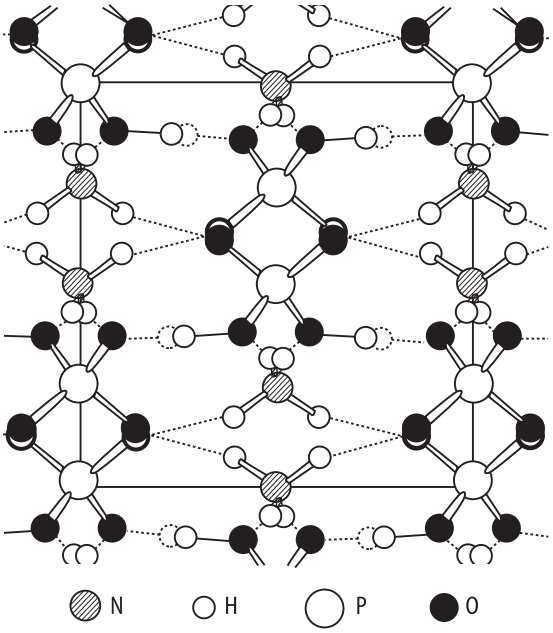

Fig. 33A-5-005. $NH_4H_2PO_4$ (ADP). Crystal structure [58Ten]. (100) projection.

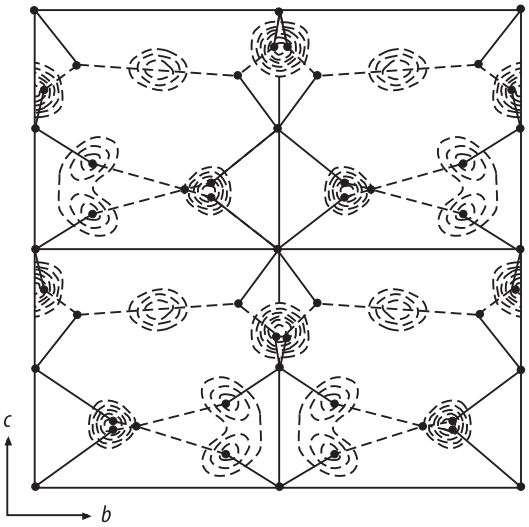

Fig. 33A-5-006. $NH_4H_2PO_4$ (ADP). Hydrogen peaks obtained by neutron difference Fourier method [58Ten]. (100) projection.

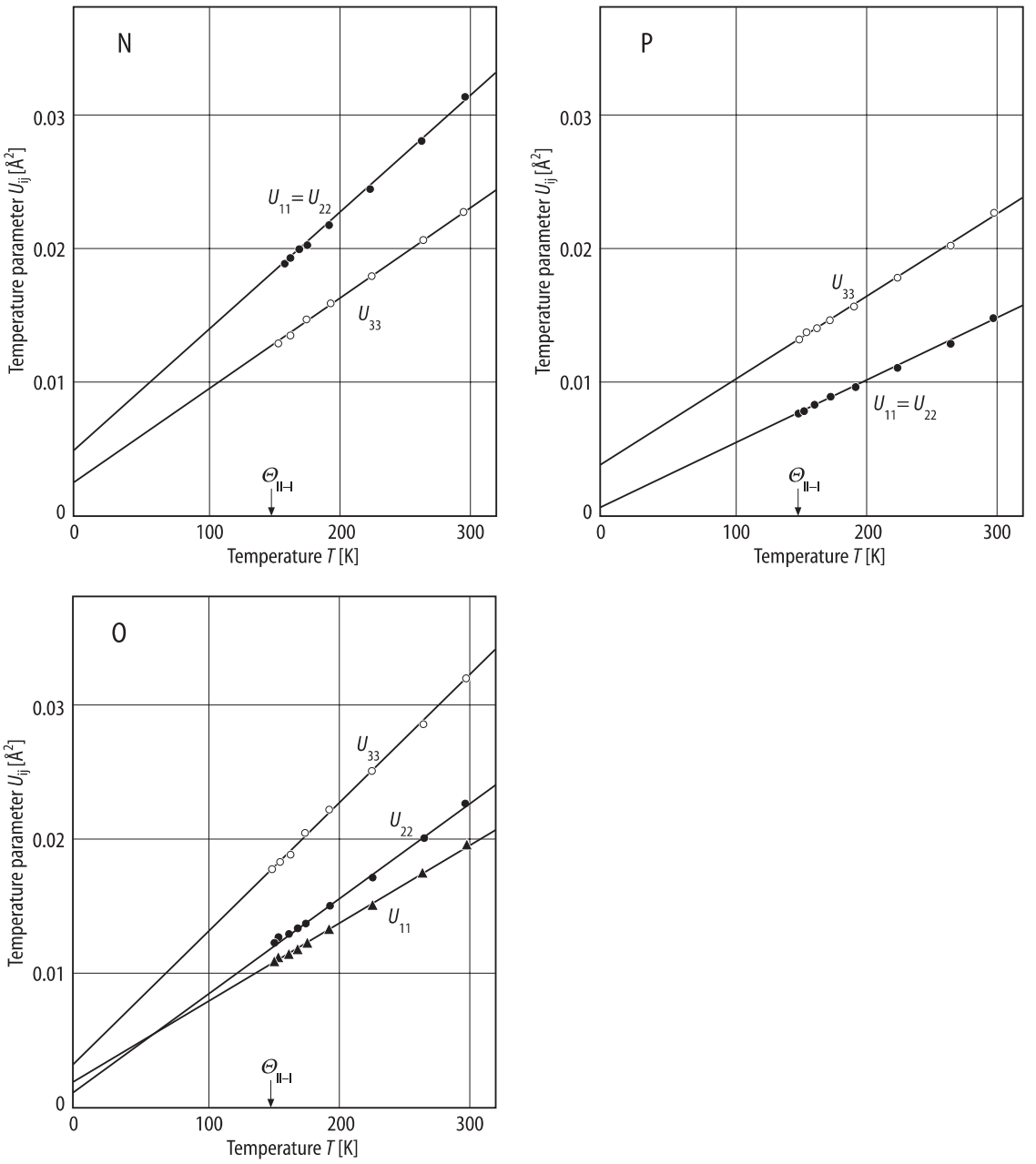

Fig. 33A-5-007. $NH_4H_2PO_4$ (ADP). U_{ij} vs. T [90Ito]. U_{ij}: anisotropic temperature parameters defined by Eq. (d) in Introduction.

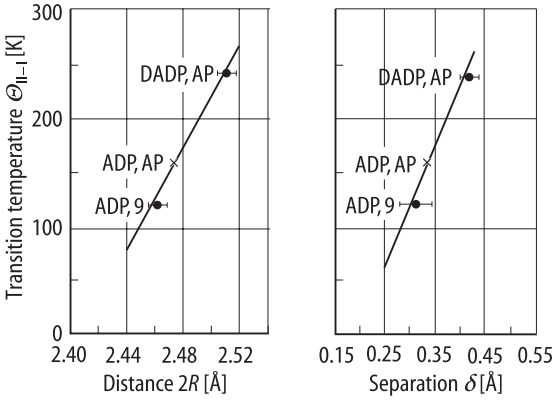

Fig. 33A-5-008. $NH_4H_2PO_4$ (ADP), $ND_4D_2PO_4$ (DADP). Θ_{II-I} vs. $2R$, δ [91Pil]. $2R$: distance between two O atoms of the hydrogen bond. δ: separation of two H sites in the hydrogen bond. AP: atmospheric pressure. 9: $p = 9 \cdot 10^8$ Pa. The data points are labelled to denote the substance and the pressure of measurement.

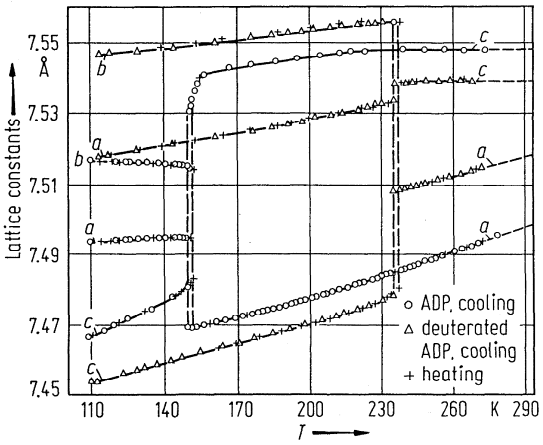

Fig. 33A-5-009. $NH_4H_2PO_4$ (ADP), $ND_4D_2PO_4$ (DADP). a, b, c vs. T [70Boi].

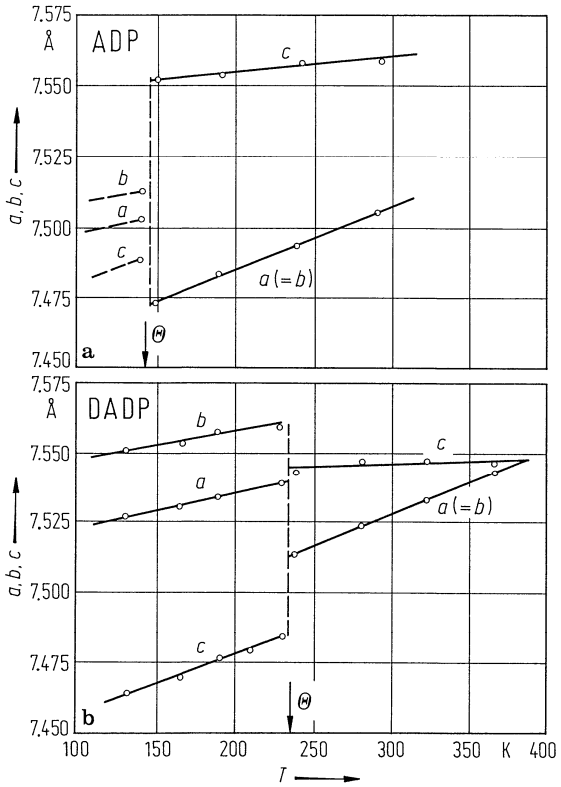

Fig. 33A-5-010. (**a**) $NH_4H_2PO_4$ (ADP), (**b**) $ND_4D_2PO_4$ (DADP). *a*, *b*, *c* vs. *T* [88Fuk2].

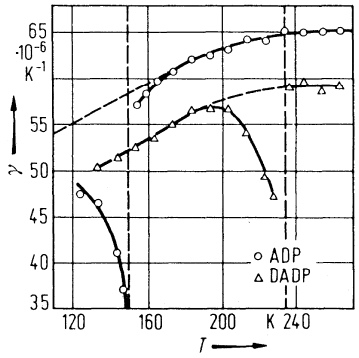

Fig. 33A-5-011. $NH_4H_2PO_4$ (ADP), $ND_4D_2PO_4$ (DADP). γ vs. *T* [70Boi]. γ: volume thermal expansion coefficient.

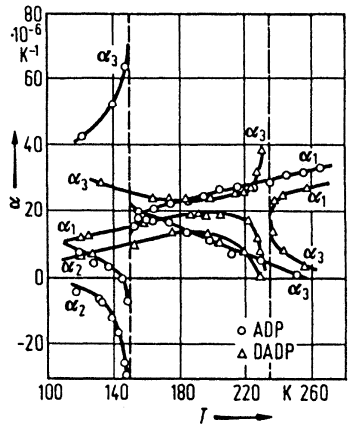

Fig. 33A-5-012. $NH_4H_2PO_4$ (ADP), $ND_4D_2PO_4$ (DADP). α vs. T [70Boi]. $\alpha = \alpha_i = \alpha_{ii}$: linear thermal expansion coefficients.

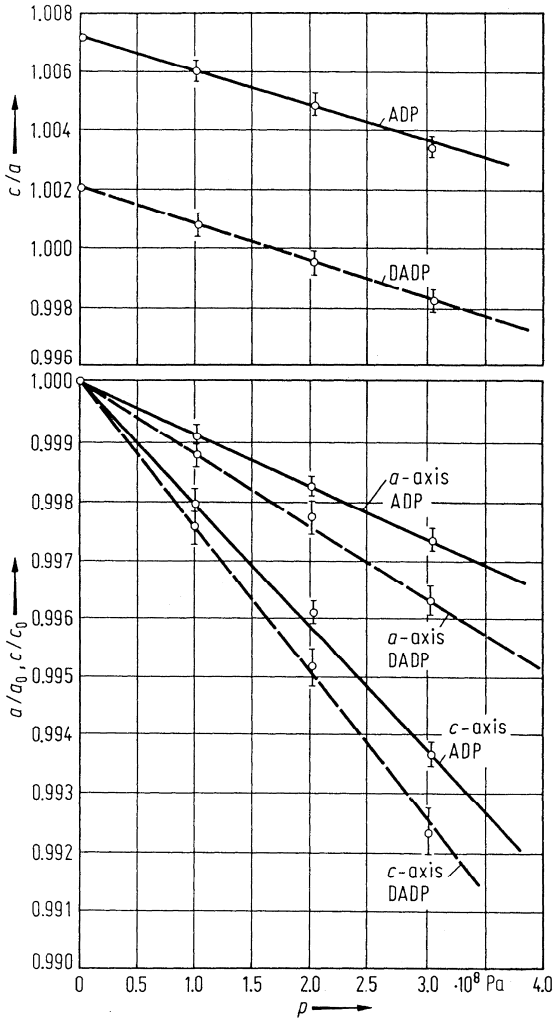

Fig. 33A-5-013. $NH_4H_2PO_4$ (ADP), $ND_4D_2PO_4$ (DADP). a/a_0, c/c_0, c/a vs. p at 295 K [71Mor]. a_0, c_0: lattice constants at atmospheric pressure.

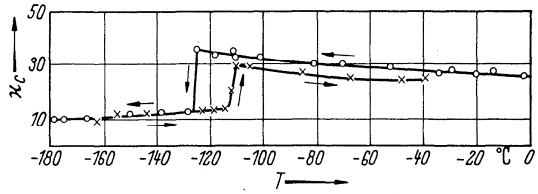

Fig. 33A-5-014. $NH_4H_2PO_4$ (ADP). κ_c vs. T [60Eis].

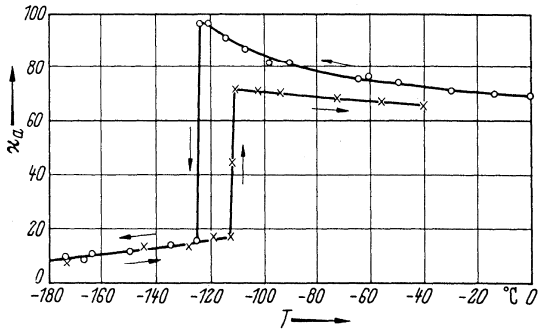

Fig. 33A-5-015. $NH_4H_2PO_4$ (ADP). κ_a vs. T [60Eis]. κ_a at f = 1 kHz.

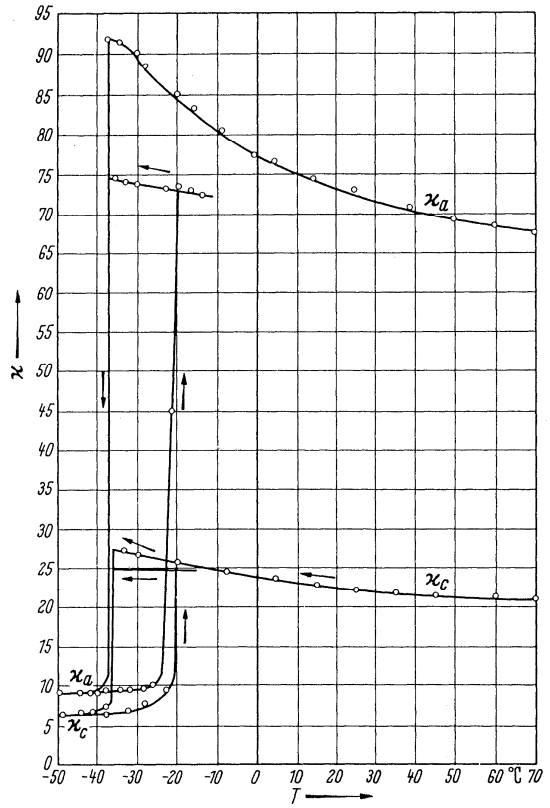

Fig. 33A-5-016. $ND_4D_2PO_4$ (DADP). κ_a, κ_c vs. T [52Mas].

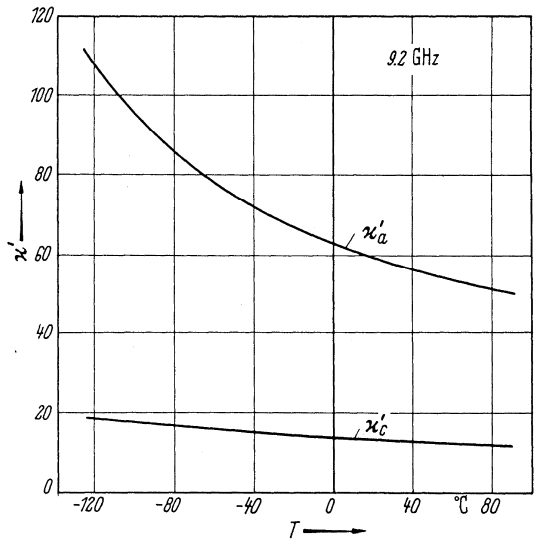

Fig. 33A-5-017. $NH_4H_2PO_4$ (ADP). κ'_a, κ'_c vs. T at 9.2 GHz [65Kam].

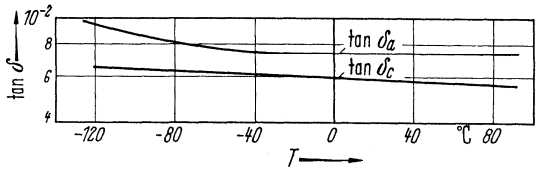

Fig. 33A-5-018. $NH_4H_2PO_4$ (ADP). tan δ vs. T at 9.2 GHz [65Kam].

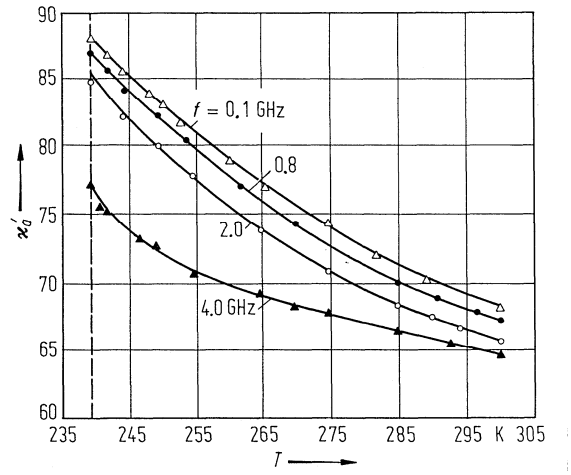

Fig. 33A-5-019. $ND_4D_2PO_4$ (DADP). κ'_a vs. T [83Jak]. Parameter: f.

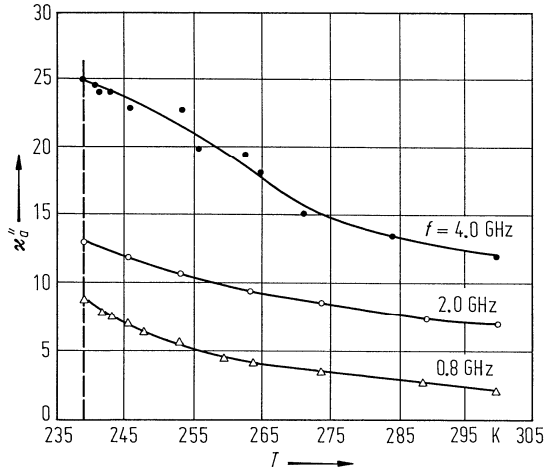

Fig. 33A-5-020. $ND_4D_2PO_4$ (DADP). κ_a'' vs. T [83Jak]. Parameter: f.

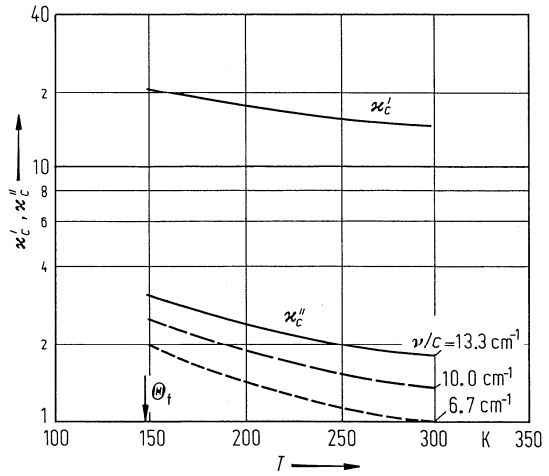

Fig. 33A-5-021. $NH_4H_2PO_4$ (ADP). κ_c', κ_c'' vs. T [80Vol]. Parameter: ν/c.

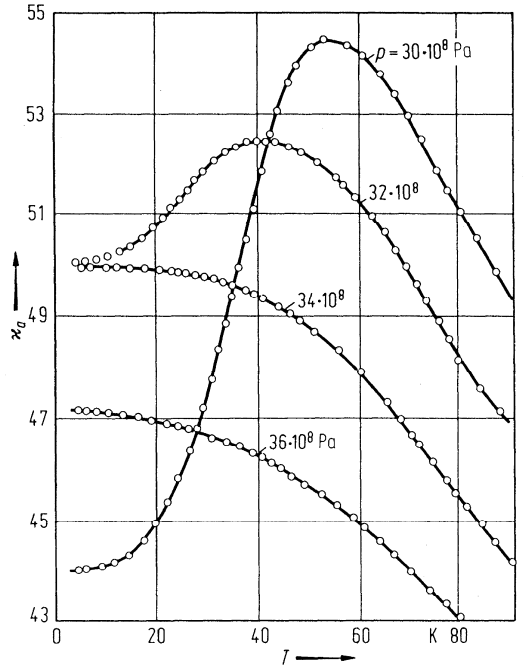

Fig. 33A-5-022. $NH_4H_2PO_4$ (ADP). κ_a vs. T [71Sam]. Parameter: p.

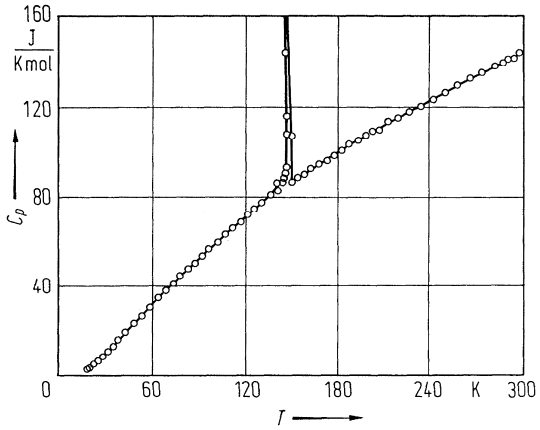

Fig. 33A-5-023. $NH_4H_2PO_4$ (ADP). C_p vs. T [44Ste]. C_p: molar heat capacity at constant pressure.

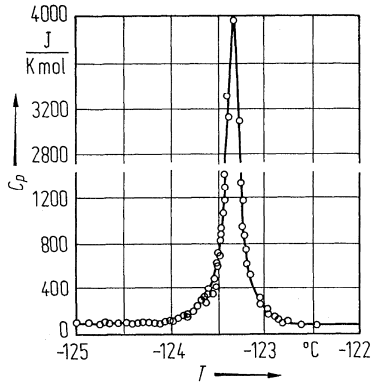

Fig. 33A-5-024. $NH_4H_2PO_4$ (ADP). C_p vs. T [70Ami]. C_p: molar heat capacity in the vicinity of Θ_{II-I}.

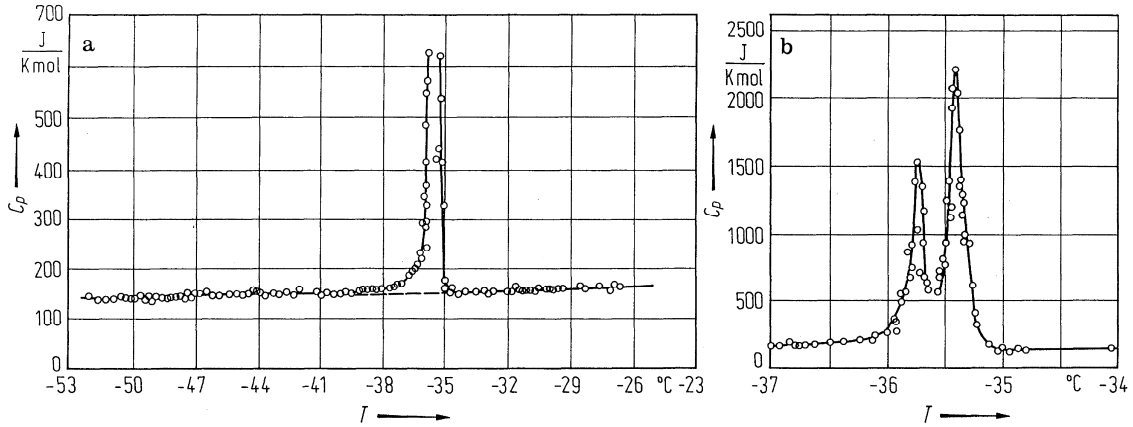

Fig. 33A-5-025. $ND_4D_2PO_4$ (DADP). C_p vs. T [70Ami]. (**a**) Wide temperature range, (**b**) in the vicinity of Θ_{I-I}.

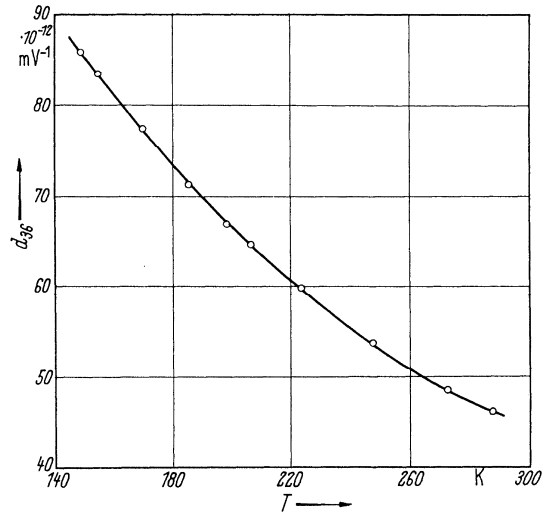

Fig. 33A-5-026. $NH_4H_2PO_4$ (ADP). d_{36} vs. T [47Mat].

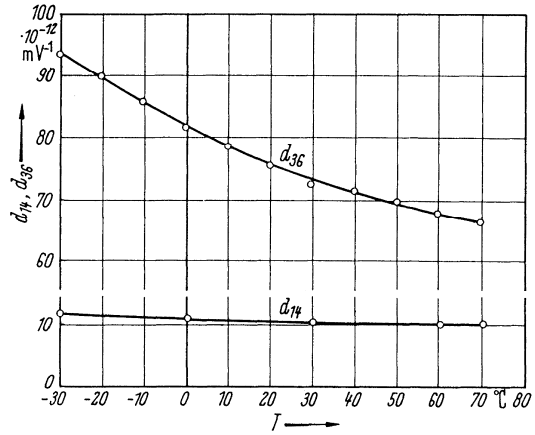

Fig. 33A-5-027. $ND_4D_2PO_4$ (DADP). d_{14}, d_{36} vs. T [52Mas].

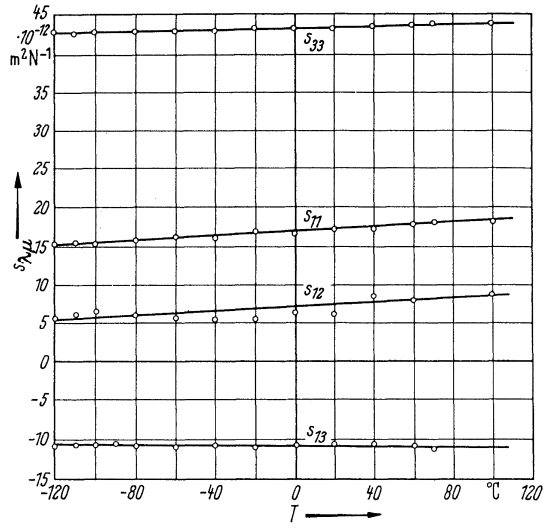

Fig. 33A-5-028. $NH_4H_2PO_4$ (ADP). $s_{\lambda\mu}$ vs. T [46Mas].

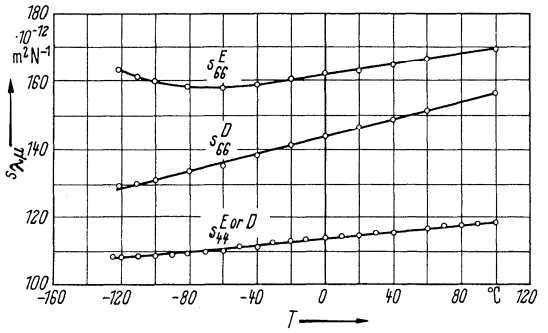

Fig. 33A-5-029. $NH_4H_2PO_4$ (ADP). s_{44}^{A}, s_{66}^{A} vs. T [46Mas]. A = ***E*** or ***D***.

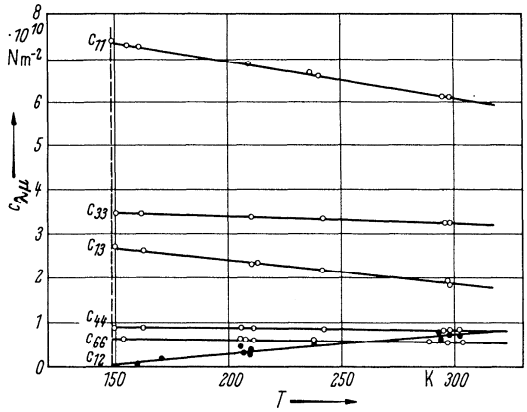

Fig. 33A-5-030. $NH_4H_2PO_4$ (ADP). $c_{\lambda\mu}$ vs. T [46Zwi].

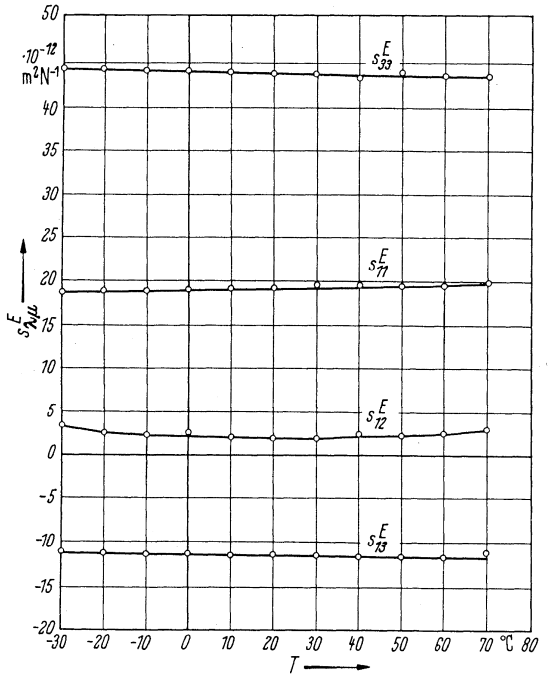

Fig. 33A-5-031. $ND_4D_2PO_4$ (DADP). $s^E_{\lambda\mu}$ vs. T [52Mas].

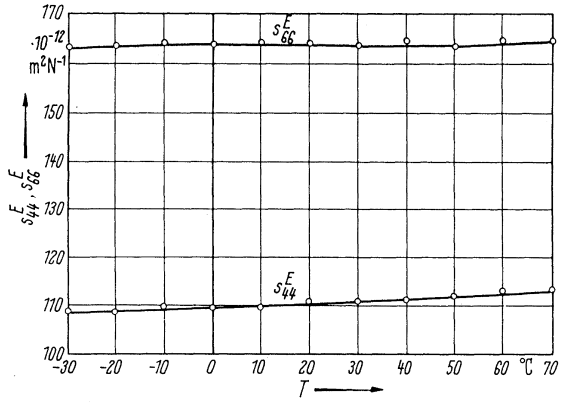

Fig. 33A-5-032. $ND_4D_2PO_4$ (DADP). s^E_{44}, s^E_{66} vs. T [52Mas].

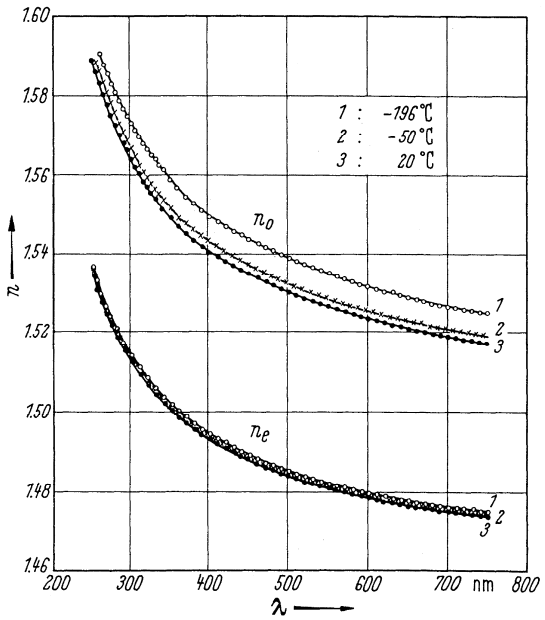

Fig. 33A-5-033. $NH_4H_2PO_4$ (ADP). n vs. λ [66Vis]. Parameter: T. See also [65Vis].

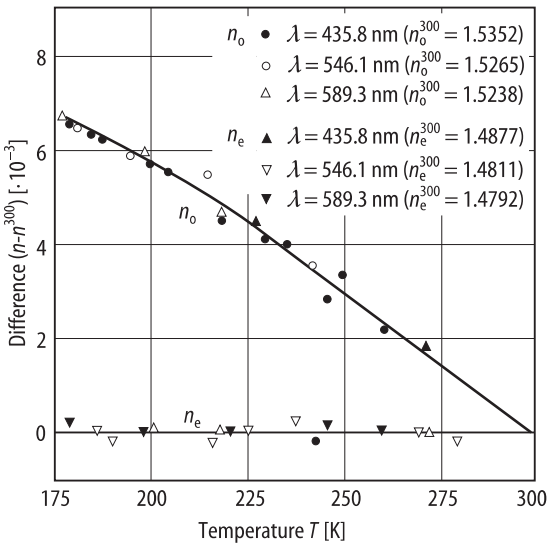

Fig. 33A-5-034. $NH_4H_2PO_4$ (ADP). ($n - n^{300}$) vs. T [66Yam]. n^{300}: refractive indices at 300 K.

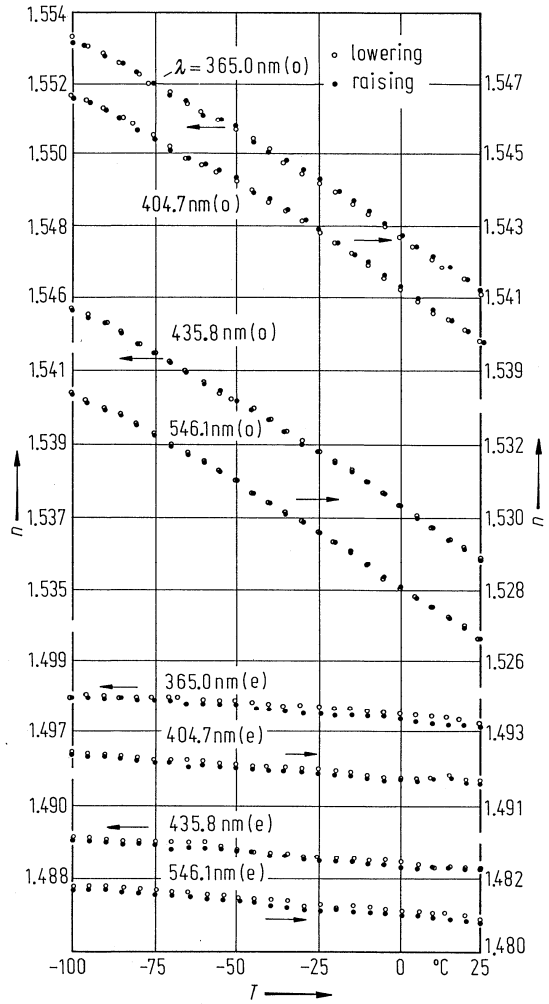

Fig. 33A-5-035. $NH_4H_2PO_4$ (ADP). n vs. T [82Ona]. Parameter: λ. o: ordinary light, e: extraordinary light.

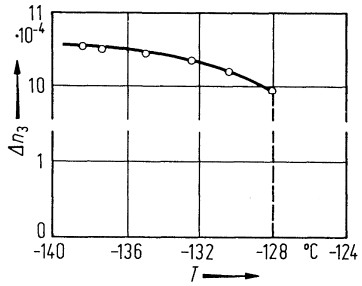

Fig. 33A-5-036. $NH_4H_2PO_4$ (ADP). Δn_3 vs. T [69Apk1]. Δn_3: birefringence in the (001) plane. $\lambda = 535$ nm.

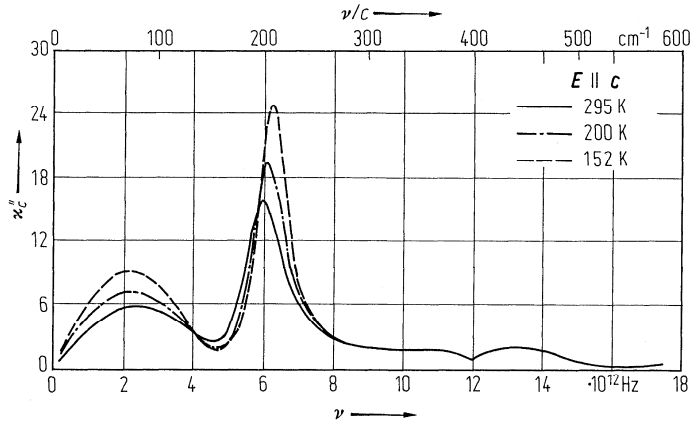

Fig. 33A-5-037. $NH_4H_2PO_4$ (ADP). κ_c'' vs. ν [73Kaw2]. Parameter: *T*. The curves were obtained from reflectivity data using Kramers-Kronig relation.

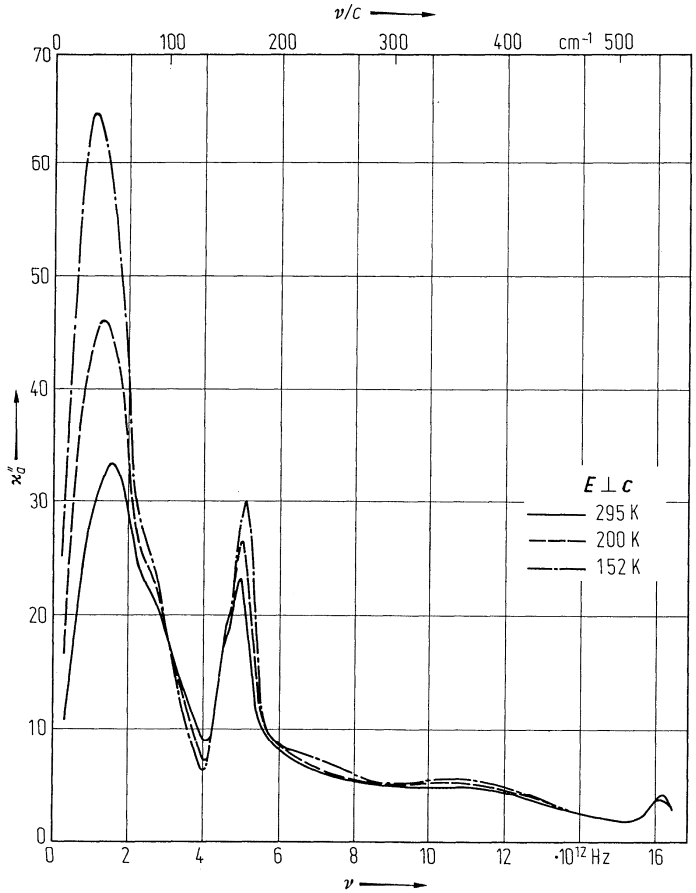

Fig. 33A-5-038. $NH_4H_2PO_4$ (ADP). κ_a'' vs. ν [73Kaw2]. Parameter: *T*. The curves were obtained from reflectivity data using Kramers-Kronig relation.

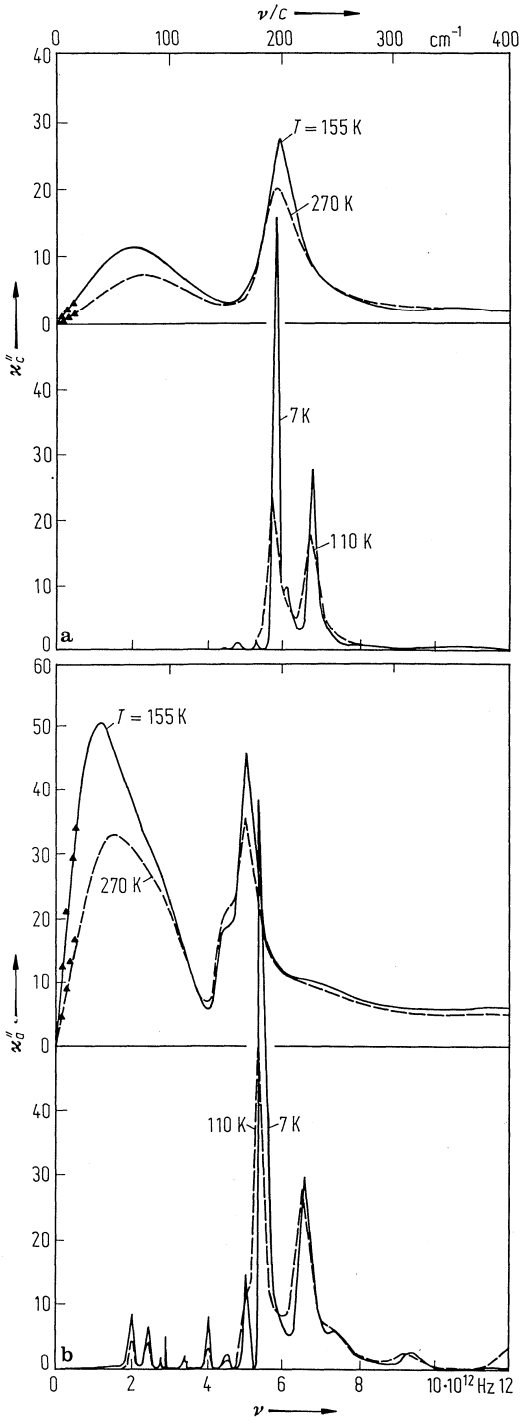

Fig. 33A-5-039. $NH_4H_2PO_4$ (ADP). κ'' vs. ν from infrared reflectivity data [86Bre]. Parameter: *T*. Full triangle: dielectric data [80Vol].

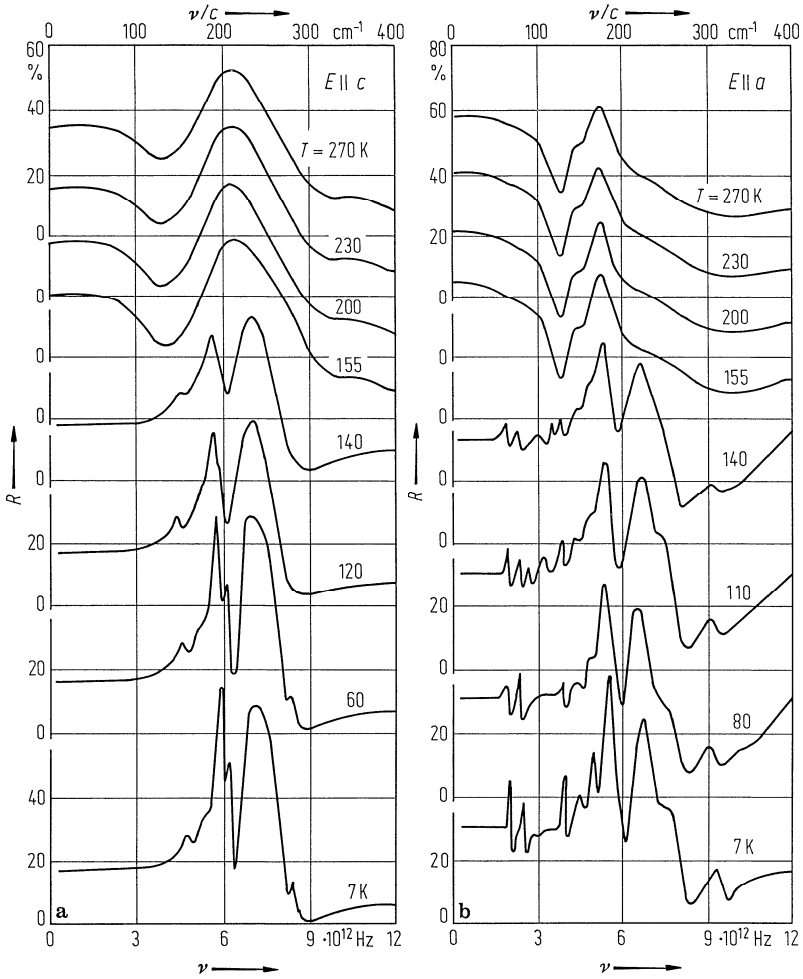

Fig. 33A-5-040. $NH_4H_2PO_4$ (ADP). R vs. ν [86Wyn]. Parameter: T. R: far-infrared reflectivity. (**a**) $\boldsymbol{E} \parallel \boldsymbol{c}$, (**b**) $\boldsymbol{E} \parallel \boldsymbol{a}$.

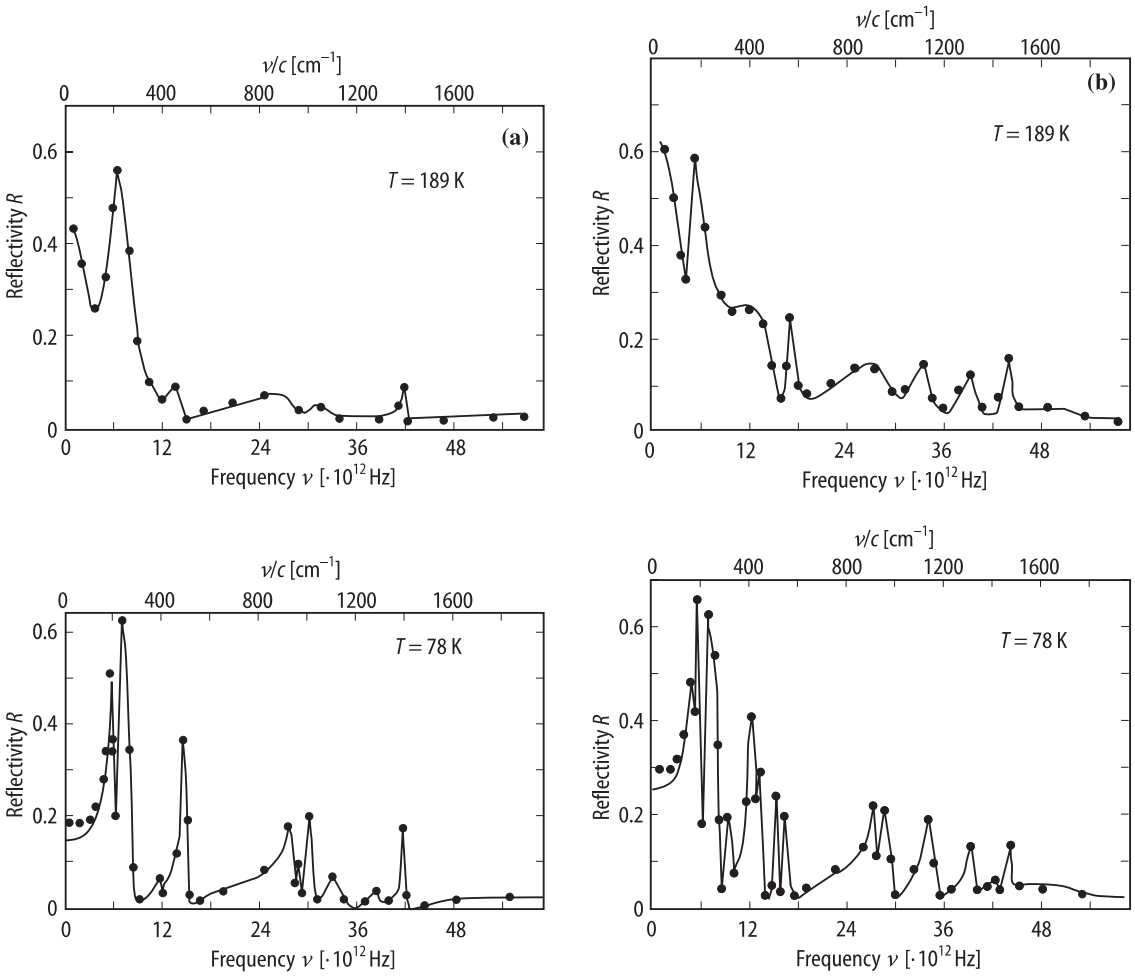

Fig. 33A-5-041. $NH_4H_2PO_4$ (ADP). *R* vs. ν [89Sim]. Parameter: *T*. *R*: far-infrared reflectivity. (**a**) $\boldsymbol{E} \parallel \boldsymbol{c}$, (**b**) $\boldsymbol{E} \parallel \boldsymbol{a}$. Full line: best fit to the factorized form of the dielectric function.

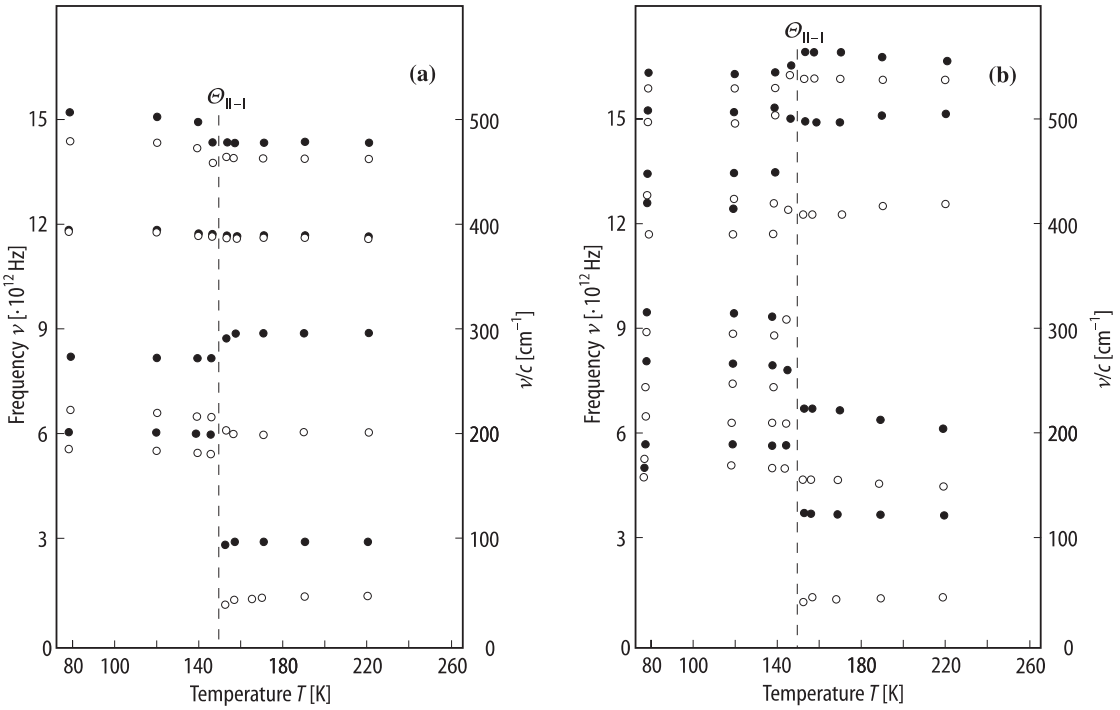

Fig. 33A-5-042. $NH_4H_2PO_4$ (ADP). ν vs. T [89Sim]. ν: optical mode frequency. (**a**) $\boldsymbol{E} \parallel \boldsymbol{c}$, (**b**) $\boldsymbol{E} \parallel \boldsymbol{a}$. Open circle: TO mode, full circle: LO mode.

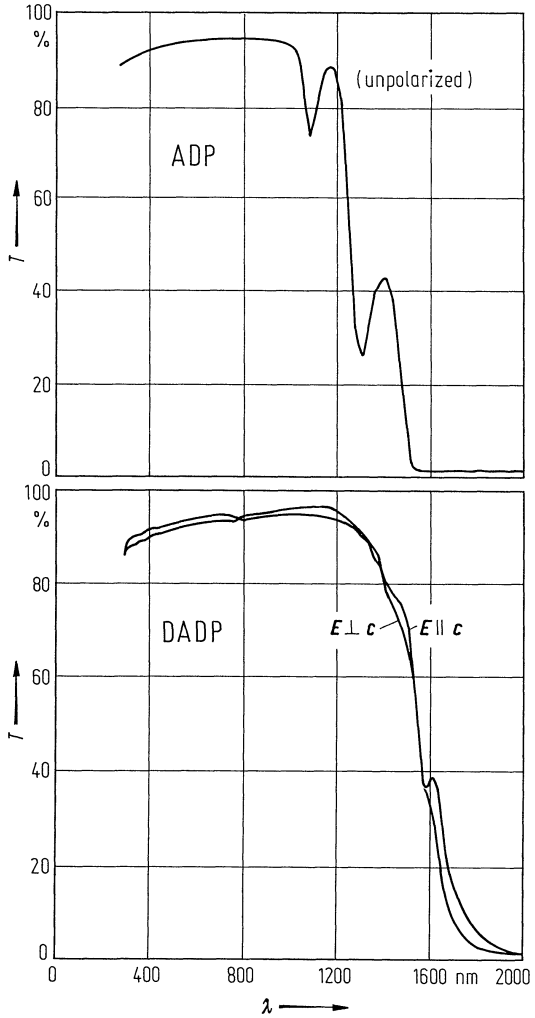

Fig. 33A-5-043. $NH_4H_2PO_4$ (ADP), $ND_4D_2PO_4$ (DADP). T vs. λ [87Eim]. T: optical transmission. Sample thickness: 11 mm.

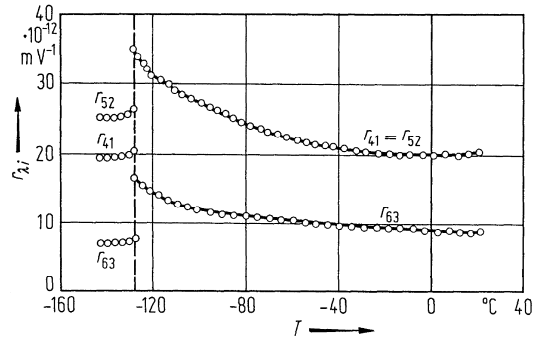

Fig. 33A-5-044. $NH_4H_2PO_4$ (ADP). $r_{\lambda i}$ vs. T [69Apk2]. r: electrooptic constant for E. $\lambda = 577$ nm.

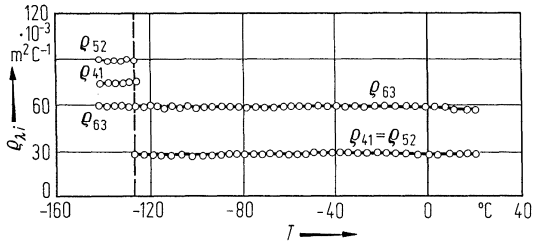

Fig. 33A-5-045. $NH_4H_2PO_4$ (ADP). $\rho_{\lambda i}$ vs. T [69Apk2]. ρ: electrooptic constant for P. $\lambda = 577$ nm.

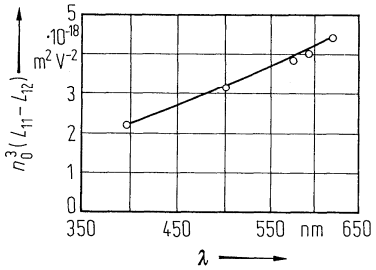

Fig. 33A-5-046. $NH_4H_2PO_4$ (ADP). $n_o^3 (L_{11} - L_{12})$ vs. λ at RT [69Apk1]. L: quadratic electrooptic constant for E.

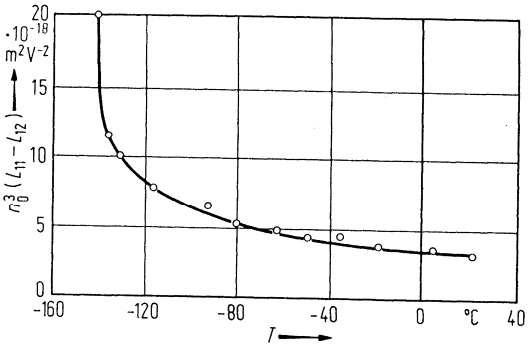

Fig. 33A-5-047. $NH_4H_2PO_4$ (ADP). $n_o^3 (L_{11} - L_{12})$ vs. T [69Apk1]. $\lambda = 518$ nm. $L_{\lambda\mu}$: quadratic electrooptic constants for E.

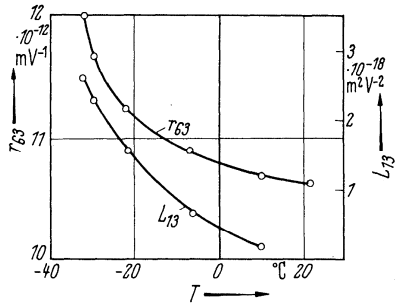

Fig. 33A-5-048. $ND_4D_2PO_4$ (DADP). r_{63}, L_{13} vs. T [66Vas]. $\lambda = 535$ nm.

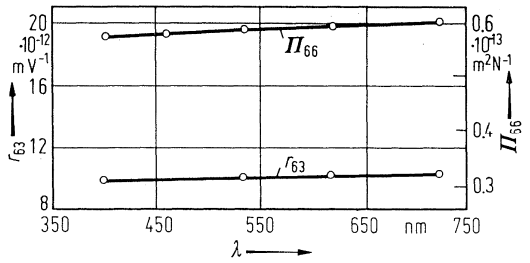

Fig. 33A-5-049. $ND_4D_2PO_4$ (DADP). r_{63}, Π_{66} vs. λ at RT [67Vas]. Π: piezooptic constant for T.

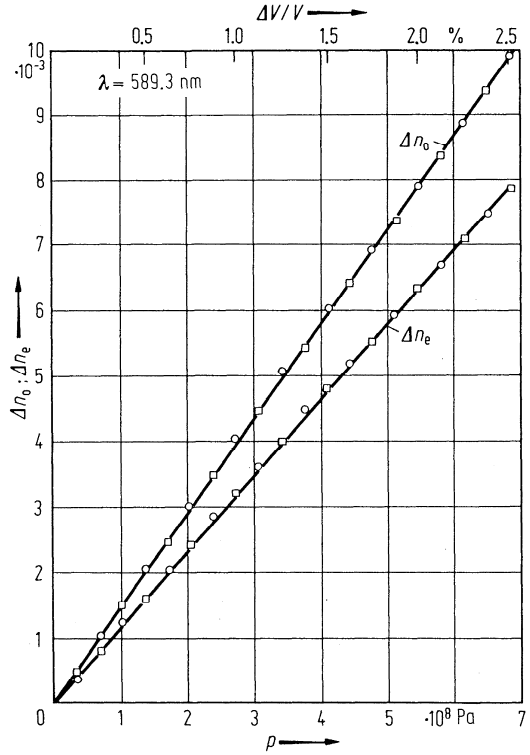

Fig. 33A-5-050. $NH_4H_2PO_4$ (ADP). Δn_o, Δn_e vs. p [68Dav]. $\Delta n_o = n_o(p) - n_o(0)$, $\Delta n_e = n_e(p) - n_e(0)$. $n_o(0) = 1.524$, $n_e(0) = 1.479$. $T = 22$ °C.

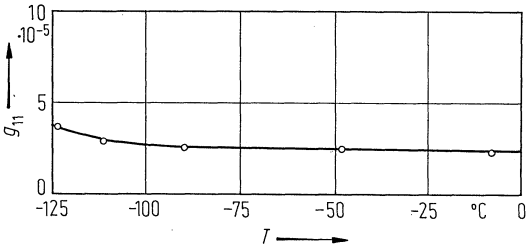

Fig. 33A-5-051. $NH_4H_2PO_4$ (ADP). g_{11} vs. T [86Vlo]. g_{11}: gyration tensor component. $\lambda = 632.8$ nm.

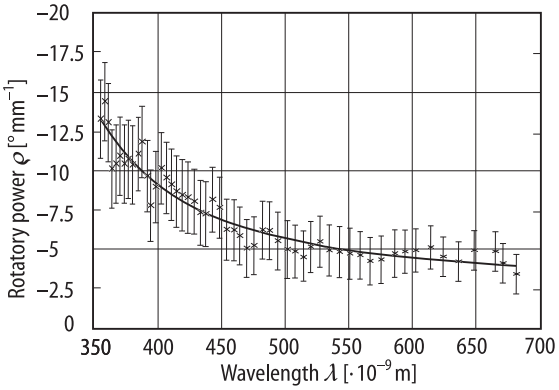

Fig. 33A-5-052. $NH_4H_2PO_4$ (ADP). ρ vs. λ [92Sta]. ρ: optical rotatory power for (100) plane. Error bars are indicated. The smooth curve is a fit to the Drude formula, $\rho = A/(\lambda^2 - \lambda_0^2) + B$.

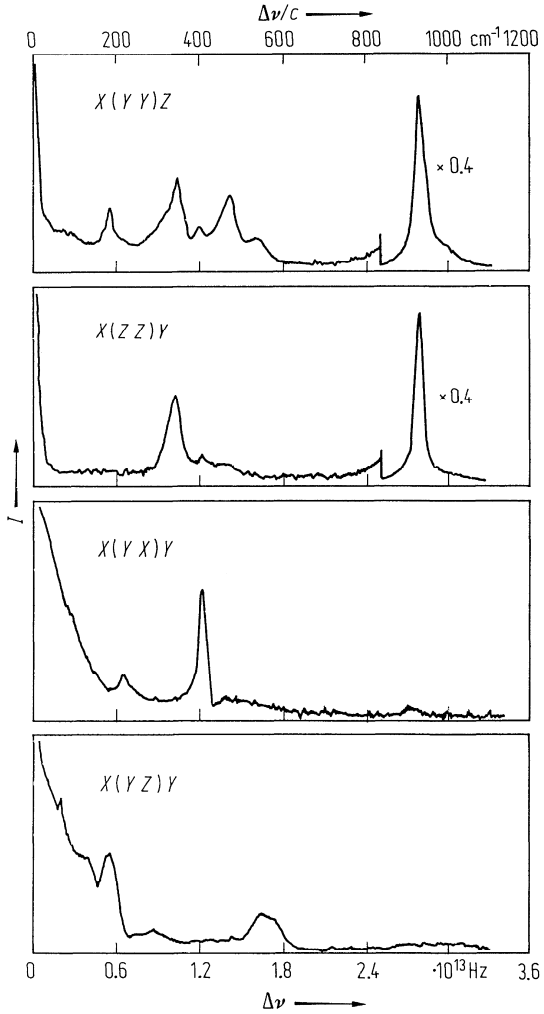

Fig. 33A-5-053. $NH_4H_2PO_4$ (ADP). I vs. $\Delta\nu$ at 295 K [73Kaw2]. I: Raman scattering intensity in different geometries.

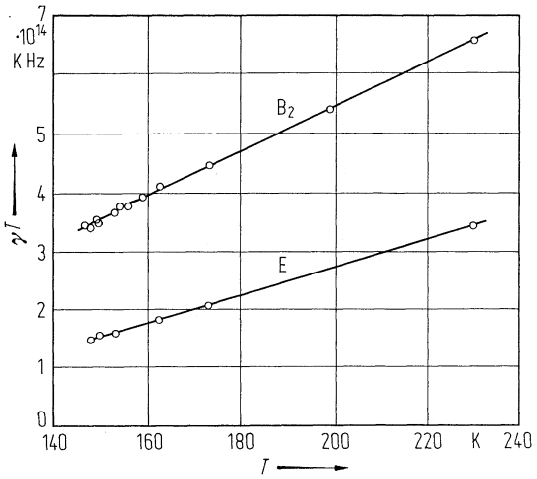

Fig. 33A-5-054. $NH_4H_2PO_4$ (ADP). γT vs. T [72Bro]. γ: inverse of the Debye relaxation time obtained from Raman spectra of a B_2 mode and an E mode. See also [72Roy].

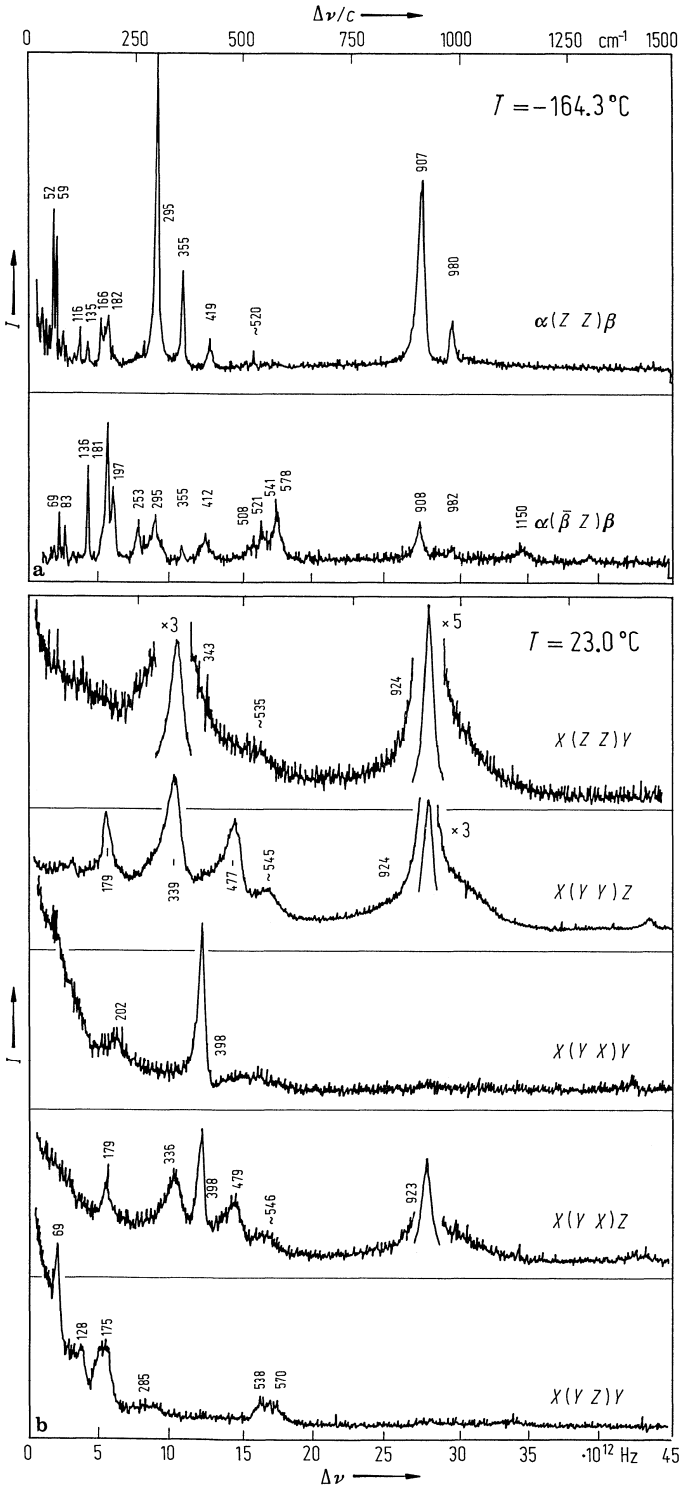

Fig. 33A-5-055. $NH_4H_2PO_4$ (ADP). I vs. $\Delta\nu$ [86Kas]. I: Raman scattering intensity. (**a**) Phase II, (**b**) phase I. α and β denote the directions inclined by 12° from the X and Y axes, respectively.

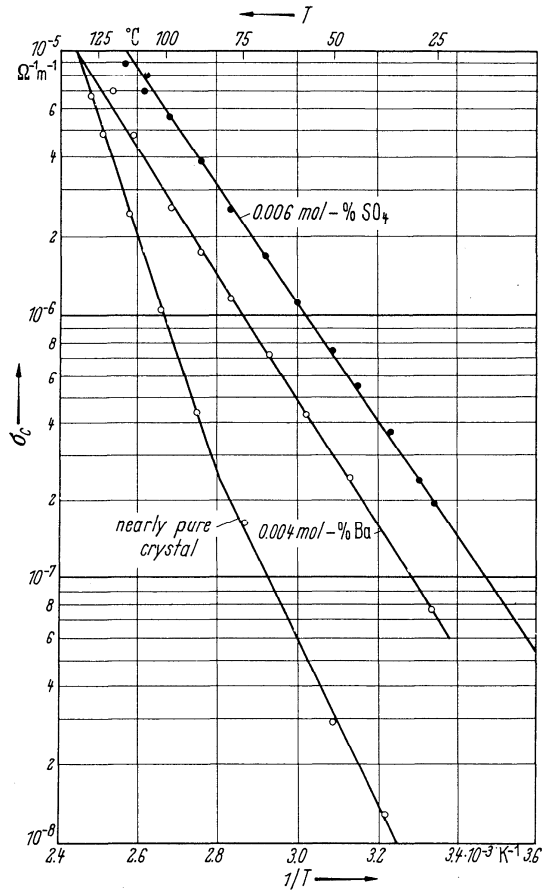

Fig. 33A-5-056. $NH_4H_2PO_4$ (ADP). σ_c vs. $1/T$ [64Mur]. σ_c: electrical conductivity along the c axis for crystals with and without impurities. Applied field: 50...180 kV m^{-1}. Specimen: $10 \times 10 \times 3$ mm^3, electrodes: Au.

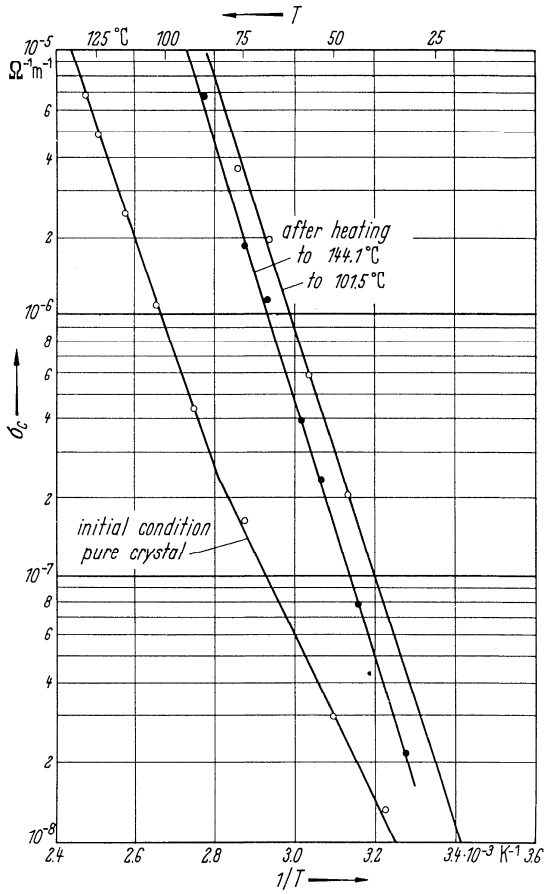

Fig. 33A-5-057. $NH_4H_2PO_4$ (ADP). σ_c vs. $1/T$ [64Mur]. σ_c: electrical conductivity along the *c* axis before and after heating for 24 hours. Measuring condition is the same as in Fig. 33A-5-056.

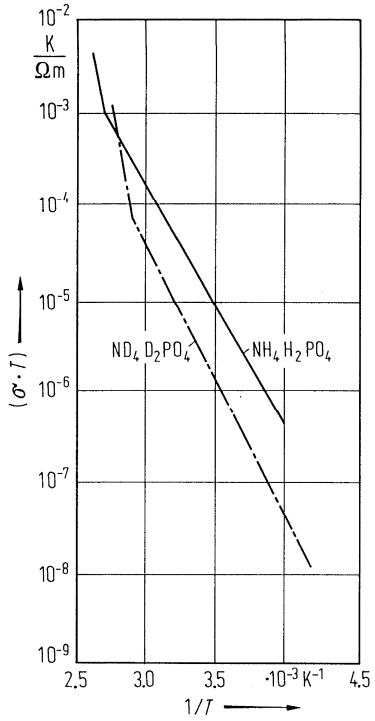

Fig. 33A-5-058. $NH_4H_2PO_4$ (ADP), $ND_4D_2PO_4$ (DADP). σT vs. $1/T$ [76Per].

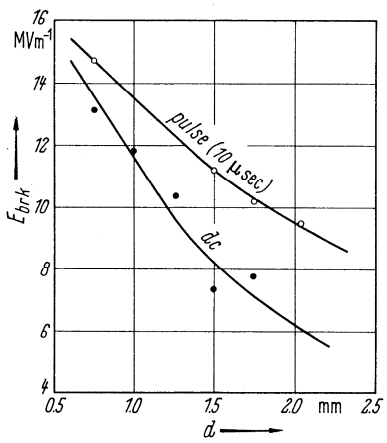

Fig. 33A-5-059. $NH_4H_2PO_4$ (ADP). E_{brk} vs. d [59Yam]. T = RT. E_{brk}: Breakdown field. d: thickness of the samples. d.c. and pulse fields are applied. Field || [001].

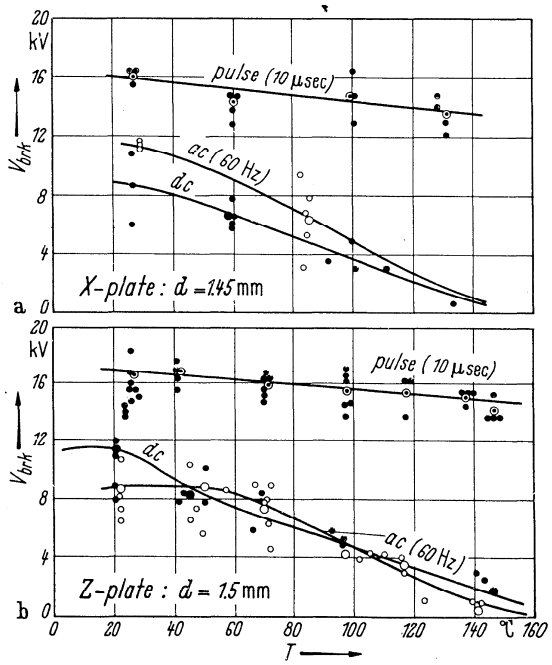

Fig. 33A-5-060. $NH_4H_2PO_4$ (ADP). V_{brk} vs. T [59Yam]. V_{brk}: breakdown voltage. d.c., a.c. and pulse (10 μs) voltages are applied. (**a**) X-plate with d = 1.45 mm; (**b**) Z-plate with d = 1.5 mm. d: thickness of the samples.

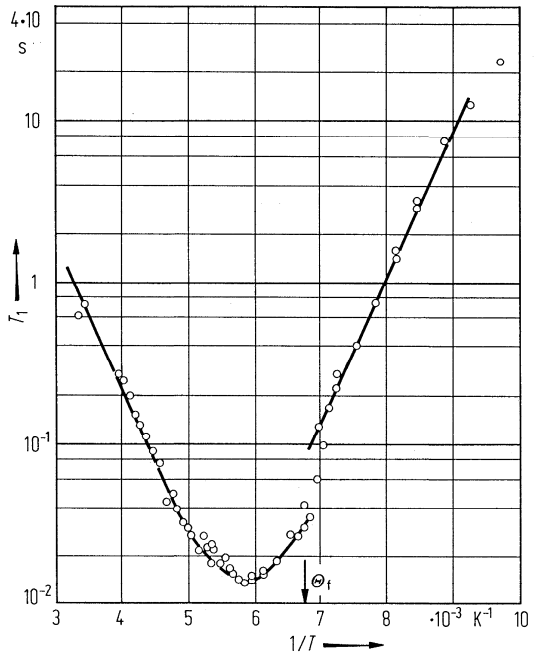

Fig. 33A-5-061. $NH_4H_2PO_4$ (ADP). T_1 vs. $1/T$ [68Gen]. T_1: proton spin-lattice relaxation time. f = 42 MHz.

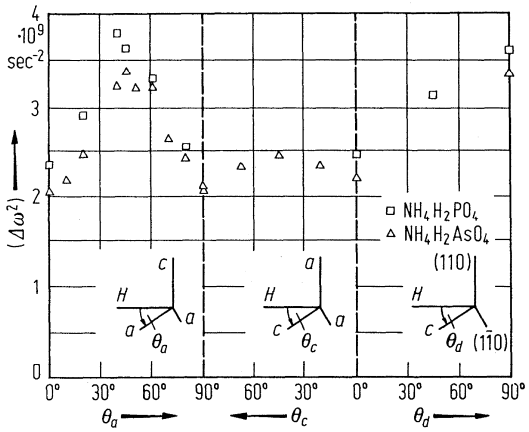

Fig. 33A-5-062. $NH_4H_2PO_4$ (ADP), $NH_4H_2AsO_4$ (ADA). $(\Delta\omega^2)$ vs. θ [71Adr]. $(\Delta\omega^2)$: second moment of proton resonance line. θ: angle between H and the crystallographic axes as shown in the figure.

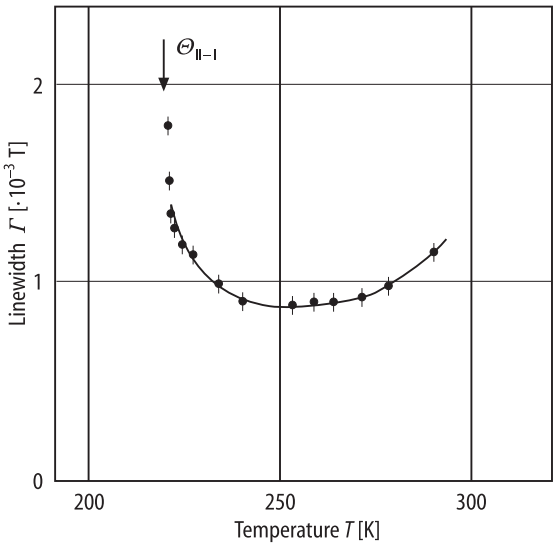

Fig. 33A-5-063. $ND_4D_2PO_4$:CrO_4. Γ vs. T [89Dal]. Γ: peak-to-peak linewidth of ESR signal for CrO_4^{3-}. $\boldsymbol{H} \parallel \boldsymbol{a}$.

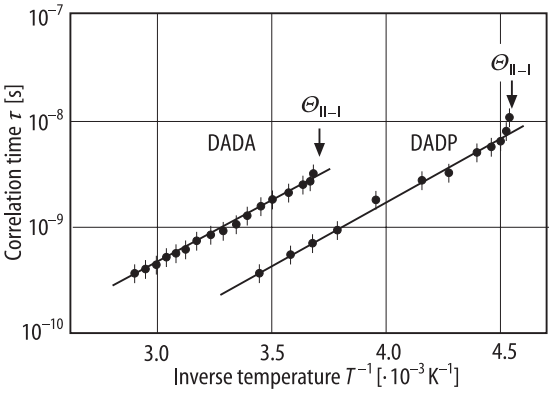

Fig. 33A-5-064. $ND_4D_2PO_4$:CrO_4, $ND_4D_2AsO_4$:CrO_4. τ vs. T^{-1} [89Dal]. τ: correlation time obtained from ESR of CrO_4^{3-} linewidth.

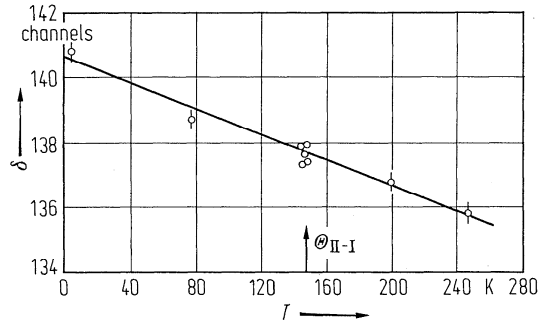

Fig. 33A-5-065. $NH_4H_2PO_4$:^{57}Fe. δ vs. T [72Sas]. δ: isomer shift. 1 channel = 0.033 mm s^{-1}.

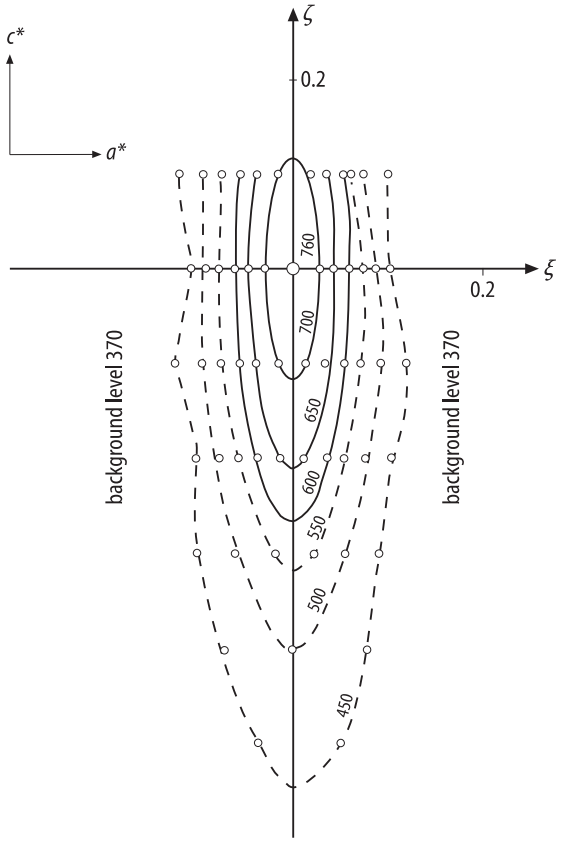

Fig. 33A-5-066. $ND_4D_2PO_4$ (DADP). Contour map of neutron diffuse scattering around (5 0 4) in the reciprocal space [69Mei]. T = 244 K.

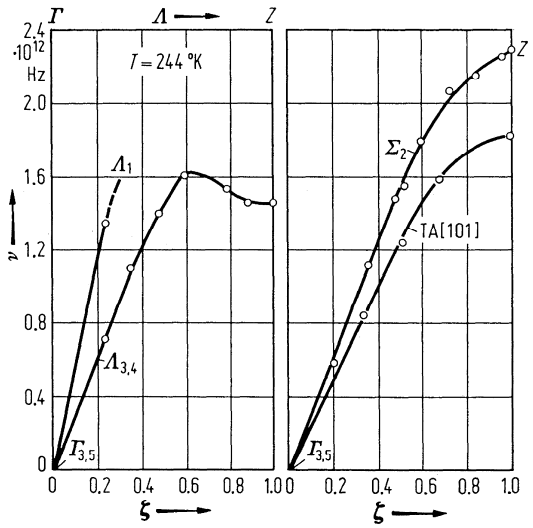

Fig. 33A-5-067. $ND_4D_2PO_4$ (DADP). ν vs. ζ [69Mei]. ν: phonon frequency. ζ: reduced wave number coordinates. For Γ, Λ and Σ, see Introduction.

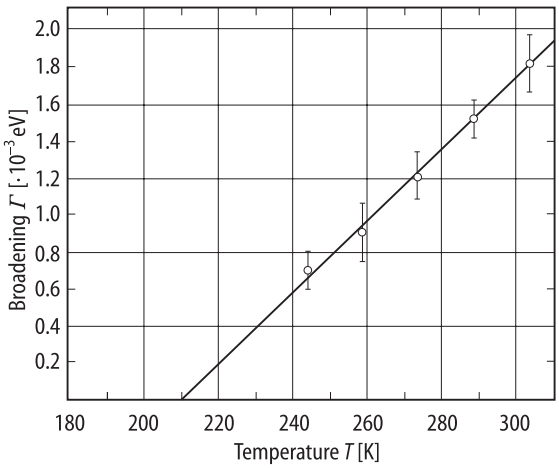

Fig. 33A-5-068. $ND_4D_2PO_4$ (DADP). Γ vs. T [69Mei]. Γ: quasi-elastic broadening of neutron scattering.